Densification of pure copper by selective laser melting process

Ken IMAI*, Toshi-Taka IKESHOJI**,
Yuji SUGITANI*** and Hideki KYOGOKU**

* Graduate School of Systems Engineering, Kindai University,
Higashi-Hiroshima, 739-2116 Japan.
E-mail: 1733850007e@hiro.kindai.ac.jp
** Fundamental Technology for Next Generation Research Institute, Kindai University,
Higashi-Hiroshima, 739-2116 Japan.
*** Fukuda Metal Foil & Powder Co.,
Kyoto, 607-8305 Japan.

Abstract

Pure copper is utilized as a material for products with complicated shape and high thermal conductivity such as heat exchangers. However, it is difficult to fabricate pure copper parts with high density by the selective laser melting (SLM) process. One of the reasons is considered to be its high thermal conductivity by which the heat in the melt pool rapidly diffuses away. Additionally, the lower rate of energy absorption of fiber laser power for pure copper makes the size of melt pool smaller. In this research, the optimum fabrication condition of high-purity 99.9% copper fabricated by SLM process was investigated by evaluating the density and microstructure. As a result, it was found that the optimum condition of laser power and scan speed are 800~900W and 300 mm/s, respectively, and the optimum energy density is around 1000 J/mm^3, which is much higher than that of other materials due to high reflectivity and high thermal conductivity of pure copper. And also, it was found that the hatch pitch is important factor to achieve the densification of the as-built specimen and the optimum hatch pitch was 0.01 mm. The high density parts were successfully fabricated by the optimum fabrication condition. The maximum density of the as-built specimen was 96.6 % and was much higher than that of the as-built part already reported.

Keywords : Additive manufacturing, Process parameter, Copper, Density, Microstructure

1. Introduction

Additive manufacturing (AM) (I. Gibson et al., 2010) is an effective technology in the industrial fields such as aerospace, medical, automotive and so on. Especially, selective laser melting (SLM) is available to fabricate a great variety of alloys such as stainless steel, titanium alloy, aluminum alloy, nickel-based superalloy and so on. However, it is difficult to fabricate the sound pure copper parts by SLM due to its high reflectivity and high thermal conductivity. Although the fabrication of pure copper has been performed by using a SLM machine with CO_2 laser (H.H. Zhu et al., 2003) (D.D. Gu and Y.F. Shen, 2006) (D. Gu et al、 2007), it was difficult to fabricate sound parts of copper because pure copper has a high reflectivity to CO_2 laser. Therefore, the densification of copper was tried to fabricate by adding copper alloy powder such as CuP and CuSn powder, but it was difficult to fabricate sound parts of copper (H.H. Zhu et al., 2003) (D.D. Gu and Y.F. Shen, 2006) (D. Gu et al.). And also copper alloy such as Cu-Cr alloy has been applied to fabricate by SLM. The high density (97.9%) Cu-Cr-Zr-Ti alloy was fabricated by SLM (A. Popovich et al., 2016). However, the high density pure copper has not been fabricated by SLM. Recently, the fabrication of pure copper has been tried using electron beam melting (EBM) (D.A. Ramires et al., 2011) (M.A. Lodes et al., 2015). Lodes et al. (M.A. Lodes

et al., 2015) reported that the pure copper with a relative density of 99.5% can be manufactured by EBM. However, it is difficult to fabricate the parts having complicated shaped cooling tubes and thin walls by EBM. Therefore, the densification of pure copper is required by SLM.

In this research, the optimum fabrication condition of high-purity 99.9% copper fabricated by SLM process was investigated with variation in laser power, scanning speed and hatch pitch by evaluating the surface morphology, density and microstructure. The surface morphology, microstructure and density of the as-built specimens were examined.

2. Experimental procedure

2.1 Specimen preparation

Gas-atomized high-purity 99.9% copper powder was prepared in this research. The mean particle diameter of the spherical powder was around 28 μm. The particle size distribution of the powder was 10~45 μm. The SEM image and chemical composition of this powder are given in Fig.1 and Table 1, respectively.

Table 1 Chemical compositions of copper powder
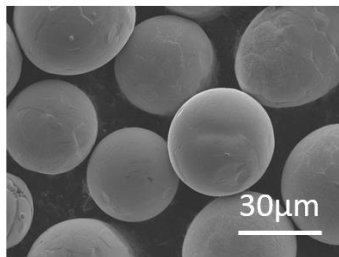
	Analysis value [mass%]
Cu	99.9
P	0.01
O	0.05

Fig.1 SEM image of pure copper powder

2.2 Procedure

A SLM machine equipped with a 1 kW single mode Yb-fiber laser was employed for fabricating the specimens on a copper base plate.

In order to examine the optimum fabrication condition, the cubic specimens with the dimension of 10x7x3 mm were fabricated under the following conditions as shown Fig.2;

- Laser power (P): 600~1000 W
- Scan speed (v): 300~1200 mm/s
- Hatch pitch (h): 0.05 mm
- Layer thickness (t): 0.05 mm
- Laser spot diameter (d): 0.1 mm
- Atmosphere: in nitrogen gas

The surface morphology was observed using a scanning electron microscope (SEM). The density of the as-built specimens was measured using not only image processing but also Archimedes method. The microstructure was observed using an optical microscope (OM). And also, the melting and solidification behavior of melt pool was observed using a thermos-viewer and a high speed camera.
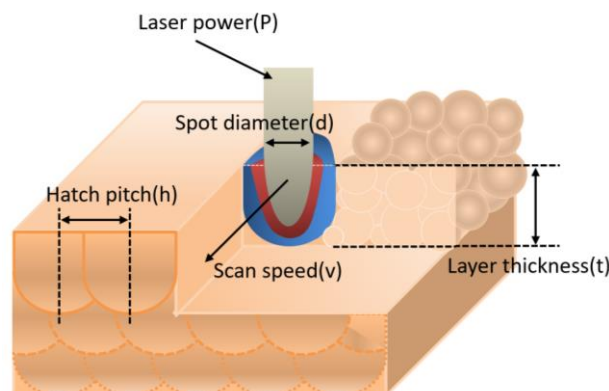

Fig.2 Schematic of the SLM process

3. Results and discussions

3.1 Investigation of the optimum laser power and scan speed

In order to manufacture the sound pure copper parts, the optimum fabrication condition was investigated. At first, the optimum condition of the laser power and the scan speed was examined by observation of surface morphology of the as-built cubic specimens. Figure 3 shows the process map between laser power and scan speed evaluated by surface morphology. As shown in this figure, the surface morphology can be roughly classified into three types as follows;

(A) a smooth surface obtained by continuous smooth tracks

(B) a rough surface obtained by instability tracks

(C) a discontinuous surface including pores obtained by Rayleigh instability

In the case of the scan speed of 300 mm/s at the laser power between 600 and 900 W and the scan speed of 600 mm/s at the laser power of 900 and 1000 W, the smooth surface was obtained. Additionally, the shape of melt pool observed using a thermo-viewer is demonstrated in Fig.3. The higher the scan speed, the rougher the surface morphology of the specimen. The size of melt pool of the lower scan speed is smaller than that of the higher scan speed as shown in Fig.4. It is thus difficult to fabricate the sound parts at higher scan speed owing to insufficient energy density and high thermal conductivity.

The quality of the SLMed part such as surface morphology and microstructure is strongly influenced by the energy density, E, calculated by the following equation;

$$E = P/vht \tag{1}$$

where P:laser power [W], v:scan speed [mm/s], h:hatch pitch [mm], and t:layer thickness [mm].

The energy densities of the surface morphology (A), (B), and (C) correspond to the followings, respectively;

(A): 600~1200 J/mm^3

(B): 311~533 J/mm^3

(C): 200~333, 1333 J/mm^3

As a result, the smooth surface of the specimen was obtained at the energy density between 600 and 1200 J/mm^3 by evaluation of surface morphology. But the swelling took place on the surface fabricated at 1000 W and 300 mm/s because of excess energy density of 1333 J/mm^3.
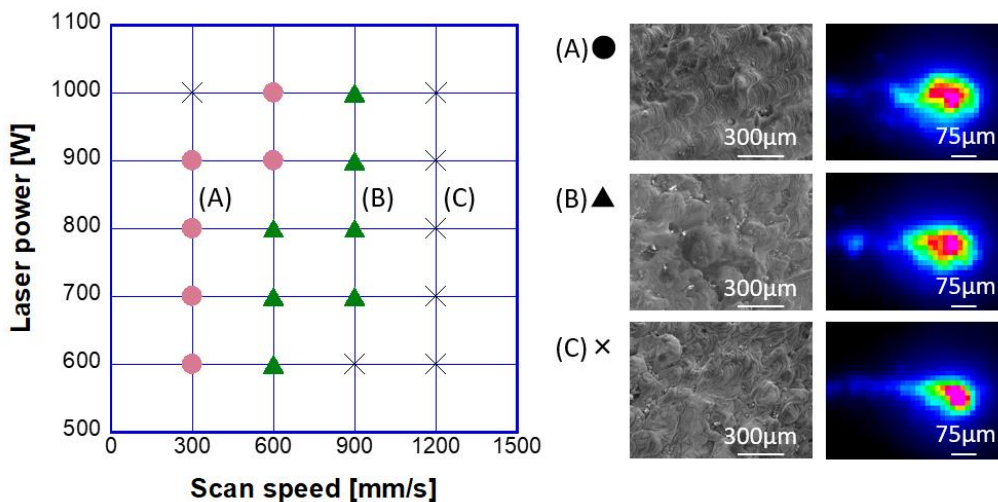

Fig.3 Process map between laser power and scan speed evaluated by surface morphology and the shape of melt pool observed using a thermo-viewer

Next, the optimum condition of the laser power and the scan speed was examined by observation of porosity of the as-built cubic specimens. Figure 4 shows the process map between laser power and scan speed evaluated by porosity in the microstructure of the cross-section of the specimen. In the case of (A), small pores can be observed in central part of the specimen. On the other hand, in the case of (C), a lot of large pores can be observed in both near surface and central
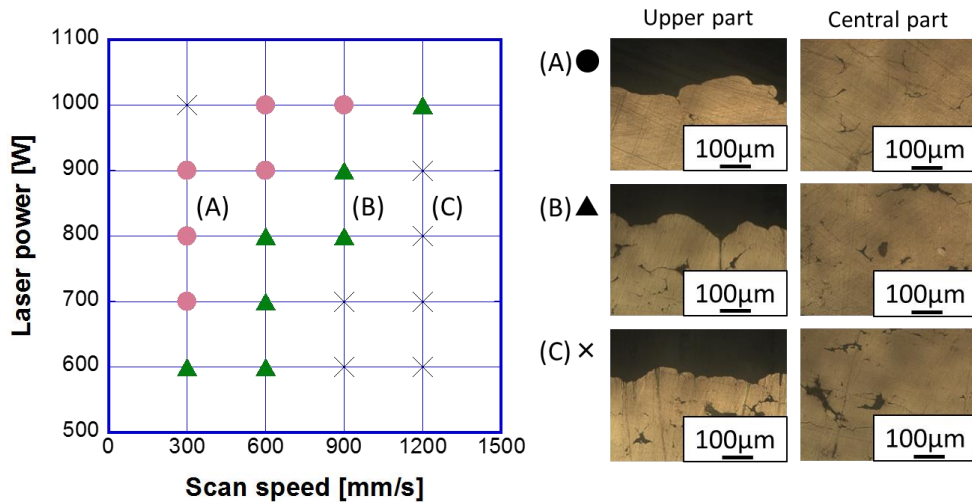
Fig.4 Process map between laser power and scan speed evaluated by porosity

part of the specimen because of insufficient melting state by lower energy density

Finally, the optimum condition of the laser power and the scan speed was examined by measurement of density of the as-built cubic specimens. Figure 5 shows the process map between laser power and scan speed evaluated by density, ρ. The rank (A), (B) and (C) correspond to the following range of the relative density, (A) 100 % $\leqq \rho \leqq$ 99 %, (B) 98 % $\leqq \rho <$ 99 %, and (C) $\rho \leqq$ 98%, respectively. The microstructure of the central part of the rank (A), (B) and (C) are almost full dense state, lack of fusion state, and porous state, respectively. The porosity increases with increasing the energy density. The range of the energy density of (C) is 200~356 J/mm^3, on the other hand, the range of the energy density of (A) is 400~1200 J/mm^3. As a result, it was found that the energy density is needed over 400 J/mm^3 to fabricate high density parts.

(A) 100 % $\leqq \rho \leqq$ 99 %, (B) 98 % $\leqq \rho <$ 99 %, and (C) $\rho \leqq$ 98%
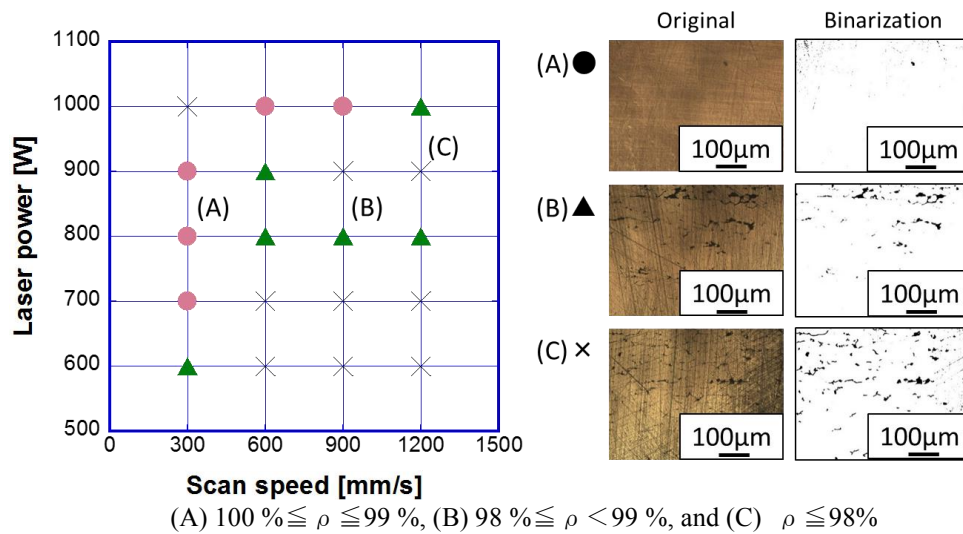
Fig.5 Process map between laser power and scan speed evaluated by density

The schematic diagram of the process map between laser power and scan speed and the energy density of the rank (A) are summarized in Fig.6 and Table 2, respectively. The quality of parts strongly depends on the energy density.

As a result from these process maps, the optimum process parameters are as follows;
- Laser power: 700~1000 W
- Scan speed: 300~600 mm/s

It is known that the optimum energy density of stainless steel, and nikel-based superalloy is around 70 J/mm^3. Thus the optimum energy density of around 1000 J/mm^3 of high-purity copper is much higehr than that of other materials. This is because high-purity copper has much higher thermal conductivity and reflectivity than that of other materials.
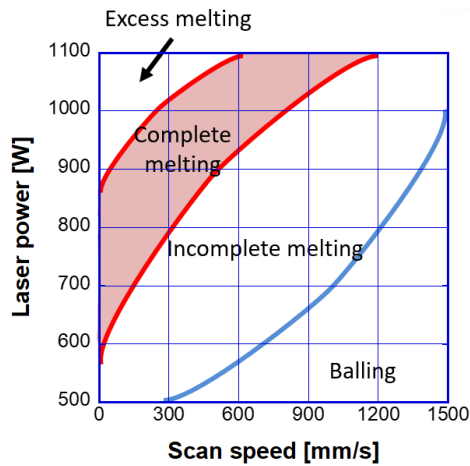
Fig.6 Schematic diagram of process map

Table 2 Energy density of the rank (A)

Laser power [W]	Scan speed [mm/s]	Energy density [J/mm^3]
1000	600	667
900	300	1200
800	300	1067
700	300	933

3.2 Microstructure of the as-built parts

The cubic specimens with the dimension of 10x10x10 mm were fabricated on a copper plate under the optimum fabrication condition. Figure 7 shows the microstructure of the as-built specimen fabricated at a laser power between 1000 and 600 W and at a constant energy density of 1000 J/mm^3. In the case of the laser power of 600 W and 700 W, lack of fusion is observed near the surface as shown in Fig.7 (a), while in the case of the laser power of 1000 W, a few small pores are observed as shown in Fig.7 (c). In the case of the laser power of 800 W and 900 W, few pores are observed as shown in Fig.7 (b). As a result, it was found that the optimum laser power is between 800 and 900 W. Figure 8 shows an example of the cubic specimens fabricated at 800 W and 900 W. The sound cubic specimens could be fabricated as shown in Fig.8.

Laser power [W]	1000	900	800	700	600
Upper part					
Central part					
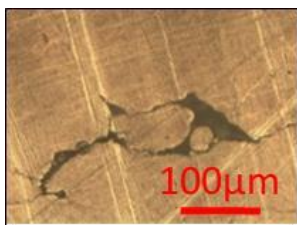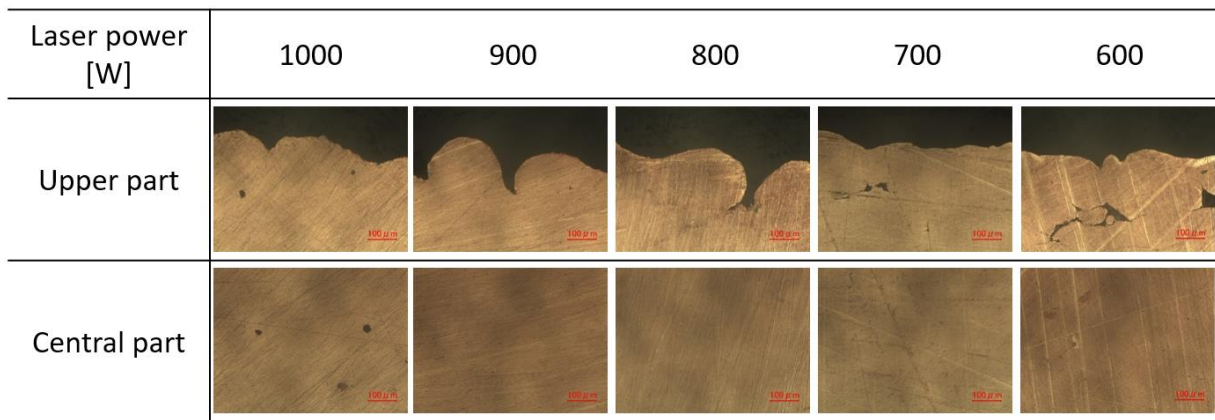
(a) Low laser power (700 W) (b) the optimum laser power (800 W and 900 W) (c) high laser power (1000 W)

Fig.7 Microstructure of the as-built specimen at various laser powers as the energy density of 1000 J/mm^3
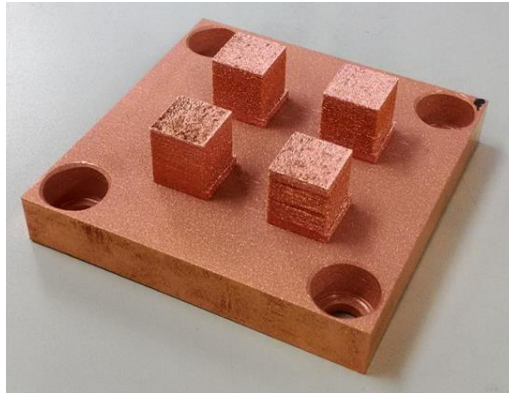
Fig.8 Cubic specimens of high-purity 99.9% copper

3.3 Investigation of the optimum hatch pitch

The effect of hatch pitch was examined between 0.025mm and 0.12 mm to improve the density of the as-built specimen. Figure 9 shows the variation in relative density as a function of hatch pitch. The relative density increases with increasing hatch pitch and shows the maximum value of 96.6 % at the hatch pitch of 0.1 mm, and then decreases. The microstructures of the as-built specimens fabricated at the scan pitch of 0.04 mm and 0.1 mm and the thermo-viewer images corresponding to the microstructures are shown in Fig.10. In case of hatch pitch 0.04 mm, a lot of pores are observed, while in the case of hatch pitch of 0.1 mm wasthe specimen is almost full dense. This may be because thermal conductivity could rapidly increase when pure copper is once in bulk state. And also, as shown in thermo-viewer image, the size of melt pool corresponding to the hatch pitch of 0.04 mm is much larger than that of the hatch pitch of 0.1 mm. Ikeshoji et al.(T.-T. Ikeshoji et al., 2018) reported that the variation of the predicted dimensions of the melt pool with time revealed instability for narrower hatch pitch and slight overlap for wider hatch pitchby the transient heat transfer analysis including melting and solidification conducted using FEM. The experimental result the hatch pitch is consistent well with the analytical one. Thus it was found that the selection of hatch pitch is important to fabricate the high densty parts.
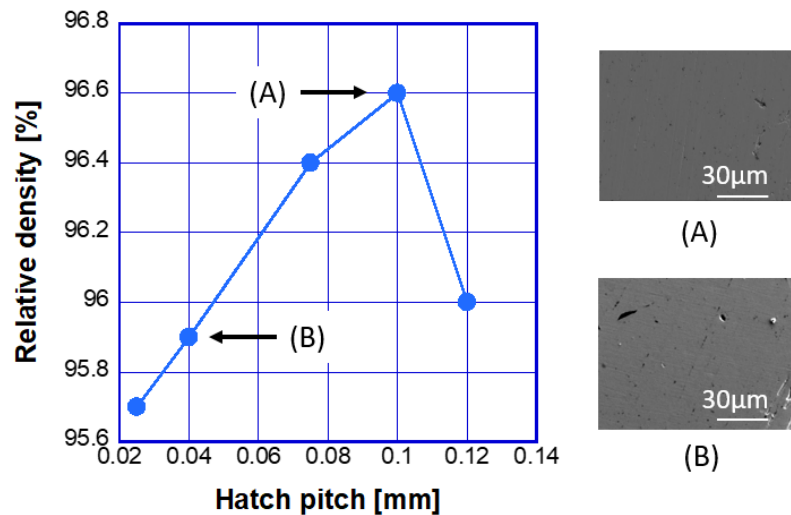

Fig.9 Relationship between relative density and hatch pitch

4. Conclusions

In this research, the optimum fabrication condition of high-purity 99.9 % copper fabricated by SLM process was investigated by evaluating the density and microstructure. As a result, it was found that the optimal process parameters of laser power, scan speed and hatch pitch are 800 W, 300 mm/s and 0.1mm, respectively. As a result, the high density parts were successfully fabricated by the optimum fabrication conditions. The maximum density of the as-built specimen was 96.6 % and was much higher than that of the as-built part already reported.
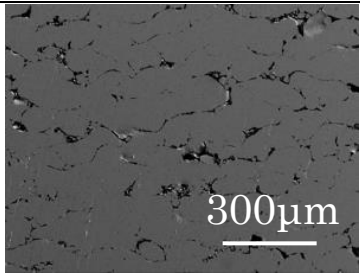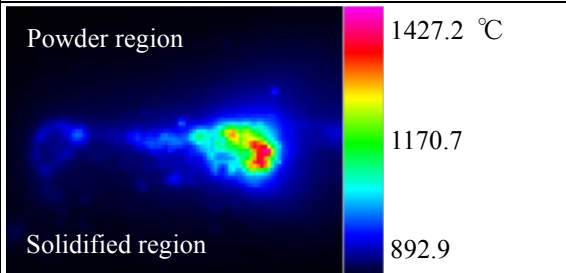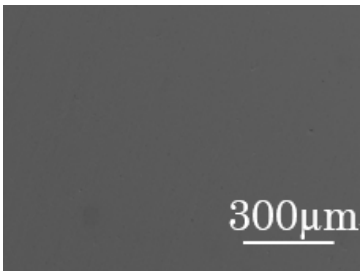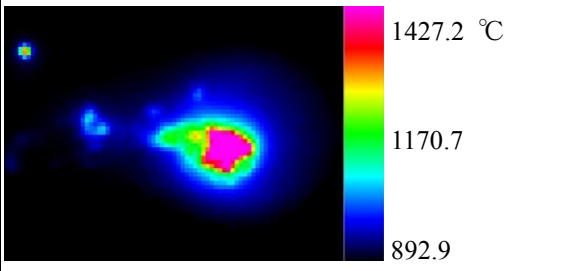
Hatch pitch [mm]	SEM image	Thermo-viewer image
0.04	300μm	Powder region / Solidified region — 1427.2 ℃ / 1170.7 / 892.9
0.1	300μm	1427.2 ℃ / 1170.7 / 892.9

Fig.10 The microstructures of the as-built specimens fabricated at the scan pitch of 0.04 mm and 0.1 mm and the thermo-viewer images corresponding to the microstructures.

Acknowledgements

References

Anatoliy A. Popovich, Vadim Sufiiarov, Igor Polozov, Evgenii Borisov, D. Masaylo, and Aleksei Orlov, Microstructure and mechanical properties of additive manufactured copper alloy, Materials Letters, Vol.179 (2016), pp.38-41.

Diana A. Ramires, Lawrence Murr, Edwin Y. Martinez, D.H. Hernandez, J.L. Martinez, Brenda I. Machado, Francisco R. Medina, Pedro Frigola, and Ryan Wicker, Novel precipitate-microstructural architecture developed in the fabrication of solid copper components by additive manufacturing using electron beam melting, Acta Materialia, Vol.59 (2011), pp.4088-4099.

Dongdong Gu and Yifu Shen, Development and characterization of direct laser sintering multicomponent Cu based metal powder, Powder Metallurgy, Vol.49 (2006), pp.258-264.

Dongdong Gu, Yifu Shen, Shangqing Fang, and Jun Xiao, Metallurgical mechanisms in direct laser sintering of Cu-CuSn-CuP mixed powder, J. Alloys and Compounds, Vol.438 (2007), pp.184-189.

Haihong Zhu, Li Lu, and Jerry Ying Hsi Fuh, Development and characterization of direct laser sintering Cu-based metal powder, Journal of Materials Processing Technology, Vol.140 (2003), pp.314-317.

Ian Gibson, David Rosen, and Brent Stucker, Additive Manufacturing Technologies, Springer, (2010).

Matthias A. Lodes, Ralf Guschlbauer, and Carolin Koerner, Process development for the manufacturing of 99.94% pure copper via selective electron beam melting, Materials Letters, Vol.143 (2015), pp.298-301.

Toshi-Taka Ikeshoji, Kazuya Nakamura, Makiko Yonehara, Ken Imai and Hideki Kyogoku, Selective Laser Melting of Pure Copper, The Journal of The Minerals, Metals & Materials Society, Vol.70 (2018), pp.396-400.